







High-efficiency reduction behavior for the oxide scale formed on hot-rolled steel in a mixed atmosphere of hydrogen and argon

Zhi-Feng Li^{1,*} , Ye Gao¹ , Guang-Ming Cao¹ , and Zhen-Yu Liu¹ 

¹ State Key Laboratory of Rolling and Automation, Northeastern University, Shenyang 110819, People's Republic of China

Received: 6 June 2019

Accepted: 11 September 2019

Published online:
17 September 2019

© Springer Science+Business
Media, LLC, part of Springer
Nature 2019

ABSTRACT

In this study, a novel double-stage reduction method of “low temperature and high temperature” was proposed to improve the reaction efficiency of the hydrogen reduction technology of the oxide scale formed on hot-rolled steel. The reduction behavior of the oxide scale in 20 vol% H₂-Ar at various reduction methods was investigated in detail. The weight change of specimen under various reduction methods was measured by thermogravimetric analysis, and then the reduction degree and the reaction rate were calculated based on the measured value. Scanning electron microscopy was used to observe the surface and the cross-sectional morphologies of the oxide scale after the reduction reaction, and the mass percent of oxygen and iron in the cross-sectional reduction layer was measured by energy-dispersive spectroscopy. X-ray diffraction was applied to characterize the phase transformation of the oxide scale in the heating process, and the phase composition of the oxide scale and reduction layer. The experimental results indicated that the reduction degree and the reaction rate of the oxide scale during the double-stage reduction method increased significantly compared with the traditional single-stage reduction method in the range of 500–800 °C. The mechanism of the double-stage reduction method was discussed from two aspects of the phase transformation of the oxide scale and the restrictive link of the gas (H₂)-solid (Fe oxides) reduction reaction.

Introduction

The oxide scale continually formed on the steel surface during the high-temperature process of hot rolling and then is removed to ensure the surface quality of the products before deep processing. Acid

pickling as a main process for removing the oxide scale from the surface of steel sheet is widely applied in the steel industry [1, 2]. However, it is inevitable that a large amount of acid waste, acid mist and liquid detergent waste are produced by the process, causing great harm to the environment.

Address correspondence to E-mail: lizhifengimust@163.com

Therefore, the hydrogen reduction technology as a new process to remove the oxide scale has been proposed. The reduction reaction is carried out in an annealing furnace in which hydrogen is used as a reducing agent to reduce the oxide scale to metallic iron, and the only waste product of the reduction reaction is water vapor. This new technology has the advantages of being both environmentally friendly protection and having a low production cost. Additionally, hydrogen energy is considered to be a type of clean and regenerative energy with the advantage of zero carbon emission, which is becoming the developmental direction of global energy. Thus, theoretical research on hydrogen reduction technology of the oxide scale that forms on hot-rolled steel sheets not only has high academic value but also will lead to the green production of steel industry in the future.

Currently, the main issue with hydrogen reduction technology for the oxide scale formed on steel sheets is that the oxide scale cannot be reduced completely in a short time due to the low reduction efficiency. The low plasticity and the high hardness of residual Fe oxides after the reduction reaction will seriously damage the surface quality of products during subsequent deep-processed such as cold rolling and hot galvanizing. [3–6] Therefore, the improvement of the reduction efficiency is not only the key to hydrogen reduction technology but also the research focus in this field both domestically and abroad [7–9].

Tanei et al. [10] investigated the effects of the initial scale structure of the hot-rolled low-carbon steel on the transformation behavior of wüstite. From this study, it is worth noting that the Fe_3O_4 layer on the outer side of the oxide scale, including the $\text{Fe}_3\text{O}_4/\text{FeO}$ double-layer structure, will be completely transformed into FeO, and then the final structure of the oxide scale was observed as a single FeO layer, when the samples were heated to 700 °C and held in N_2 for 30 min. These results suggested that the phase transformation of the oxide scale took place during the heating or isothermal stage of the reduction reaction. Chen et al. [11] systematically studied the reduction kinetics of the oxide scale with different structures on the surface of the hot-rolled low-carbon steels in 5% $\text{H}_2\text{-N}_2$, and the reduction rate of the oxide scale was the fastest with higher proportion of eutectoid structure. It can be seen that the structure of the oxide scale can determine the reduction reaction rate. However, the influence of the mechanism of the phase transformation of the oxide scale on the

reduction reaction is not clear. It is necessary to consider these factors in further research.

Meanwhile, the structural changes in the reduced iron layer during different reduction procedures as another key aspect of the hydrogen reduction in the oxide scale were researched. Saeki et al. [12] examined the reduction kinetics of the oxide scale formed on hot-rolled low-carbon steel sheets at a temperature range of 400–800 °C in pure H_2 . The results of this research revealed that the reduction efficiency presented a significantly low valley at 550–700 °C due to the structure of the reduced pure iron layer changing from porous to dense. Moukaussi et al. [13] studied the isothermal reduction process of FeO single crystals and found that the reduction rate was the lowest at 700 °C, which was attributed to the dense-reduced pure iron layer hindering the diffusion of hydrogen and water vapor. Interestingly, a previous study conducted by our research team also obtained similar results to those of Saeki et al. and Moukaussi et al. [14]. Guan et al. [15] investigated the reduction process of the oxide scale in 20% $\text{H}_2\text{-Ar}$ at a temperature range of 370–550 °C, and the reduction products were all porous iron. The pores in the reduction layer can provide channels for the diffusion of gas reducing agents and reaction products, which results in an increase in the reduction reaction efficiency with the increasing temperature in this relatively low temperature range. In 2015, the evolution of reduced iron structures formed on the stainless steel after the reduction reaction of the oxides with hydrogen was examined by Badin et al. [16]. It could be seen that the reduction products began to nucleate and grow with the prolongation of reaction time, and then their structures changed gradually from elongated pores to larger and rounder pores and then to micrometer scale porosity, which indicated that the microstructures of the reduction layers would distinctly change during different steps of short durations. Consequently, the precise controlling of the reduction layer structure by optimizing the reduction process parameters is beneficial to improving the reduction reaction efficiency.

In a previous study, we tried to add a pretreatment process to destroy the dense structure of the oxide scale before reduction reaction, thereby increasing the specific surface area of “gas–solid” phases through the formation of micro-cracking [17, 18]. This method could enhance the reduction reaction efficiency to a certain extent; however, it failed to

completely reduce the oxide scale, and residual massive oxides were still observed in the reduction layer after short reaction time.

In the current study, a novel double-stage reduction method of “low temperature and high temperature” was proposed based on previous studies. The purpose of the novel method was to combine the advantages of the reduction layer structure in gas internal diffusion and the reduction reaction of the gas–solid interface under different reduction temperatures. This paper presented a comparison of the reduction behavior of the oxide scale formed on hot-rolled low-carbon steel during the traditional single-stage method and the novel double-stage method in 20% H₂–Ar at a temperature range of 500–800 °C; the associated reaction mechanism was discussed.

Materials and methods

In the present work, the chemical composition of the hot-rolled low-carbon steel sheet was 0.045C–0.4Mn–0.05Si (wt%). The experimental specimens were sectioned to a size of 6 × 15 mm for the reduction reaction. Moreover, all specimens were cleaned with alcohol prior to the experiments. The reduction reaction of the oxide scale was conducted in a SETARAM thermogravimetric analysis (TGA) apparatus. Figure 1 shows a schematic illustration of the laboratory apparatus, and the apparatus was composed of the following parts: a vacuum, a cooling system, a temperature control system and an electronic balance with a sensibility of 30 µg.

Two reduction methods were proposed: single-stage reduction and double-stage reduction; the reduction time of the two methods was 10 min, and the experimental procedure process is shown in Fig. 2. In the method of single-stage reduction, Fig. 2a shows the furnace chamber which was filled with Ar after evacuation and then heated from room temperature to the target temperature (500, 600, 700, 800 °C) at a rate of 60 °C/min; then, the atmosphere of the furnace was immediately replaced by the synthetic atmosphere 20% H₂–Ar with a flow rate of 100 mL/min. The specimen was isothermally reduced in 20% H₂–Ar for 10 min while the weight change was recorded by the program software through the electronic balance, and then the specimen was cooled to room temperature at a rate of 40 °C/min in Ar.

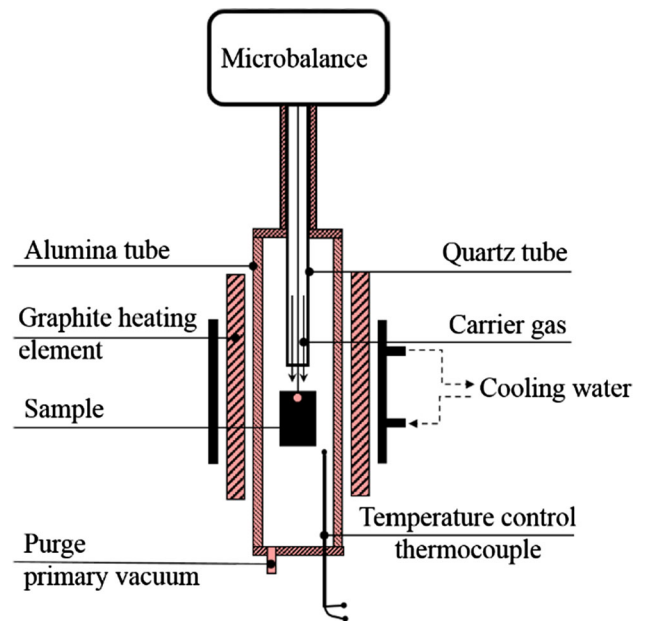


Figure 1 Schematic illustration of laboratory apparatus used for reduction reaction.

Figure 2b shows the experimental process of the double-stage reduction. The specimen was heated from room temperature to 500 °C in Ar and held in 20% H₂–Ar for the preinstalled time (1, 2, 3, 4, 5, 6 min). Subsequently, the specimen was heated to 800 °C at a rate of 100 °C/min and held for the remaining time (6, 5, 4, 3, 2, 1 min) in 20% H₂–Ar. At last, the specimen in Ar reached room temperature at a cooling rate of 40 °C/min. The weight change of the samples under different reduction methods as a function of time was measured by the electronic balance in the TGA. In the following descriptions, for convenience, the above categories of the reduction methods are given in Table 1.

The surface and cross-sectional morphologies of the oxide scale and the reduction layer were characterized by scanning electron microscopy (SEM). The oxygen weight percentage on the cross section of samples after the reduction reaction was measured by energy-dispersive spectroscopy (EDS), and then the phase composition was identified by X-ray diffraction (XRD) with a Cu-K α radiation (40 mA, 30 kV) at a scanning rate of 6°/min from 20° to 80°.

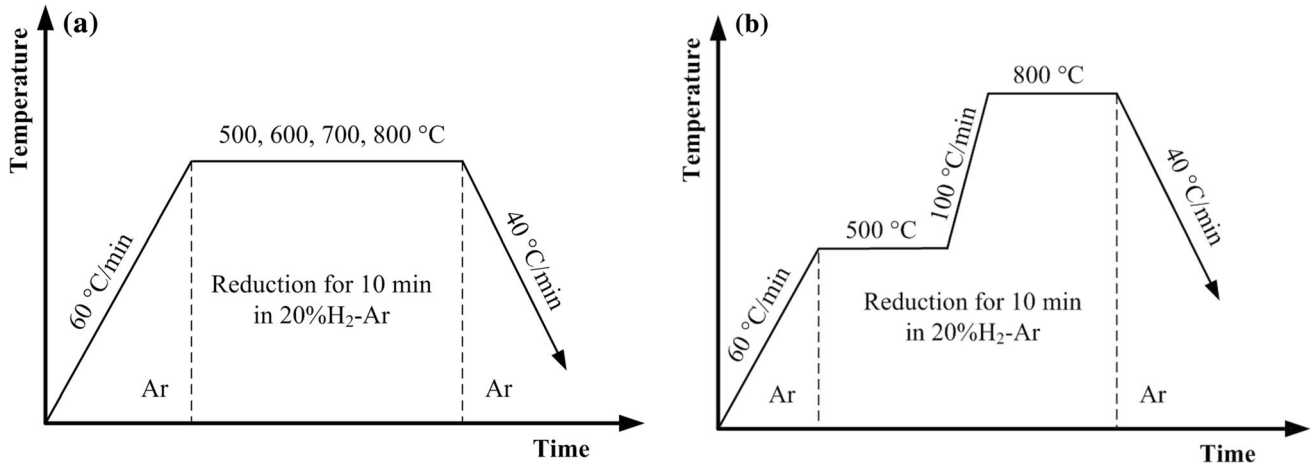


Figure 2 Schematic illustrations of different reduction methods: **a** single-stage reduction and **b** double-stage reduction.

Table 1 Symbols used for reduction experiments

Symbol	Isothermal reduction time	Symbol	Isothermal reduction time
S1	500 °C-10 min	D2	500 °C-2 min, 800 °C-5 min
S2	600 °C-10 min	D3	500 °C-3 min, 800 °C-4 min
S3	700 °C-10 min	D4	500 °C-4 min, 800 °C-3 min
S4	800 °C-10 min	D5	500 °C-5 min, 800 °C-2 min
D1	500 °C-1 min, 800 °C-6 min	D6	500 °C-6 min, 800 °C-1 min

Results

Phase composition and morphology of the oxide scale

Figure 3a shows the phase composition of the initial oxide scale formed on the hot-rolled low-carbon steel sheet and that they contain Fe_3O_4 and α -Fe. Their cross-sectional morphology is shown in Fig. 3b; the thickness of the oxide scale is 6.7 μm , and it can be

found that the oxide scale is mostly formed by Fe_3O_4 and a lamellar eutectoid structure ($Fe_3O_4 + \alpha$ -Fe). In the lamellar structure, the white layers are α -Fe and the dark gray regions are Fe_3O_4 . The structure of the initial oxide scale is similar to previous studies [19, 20].

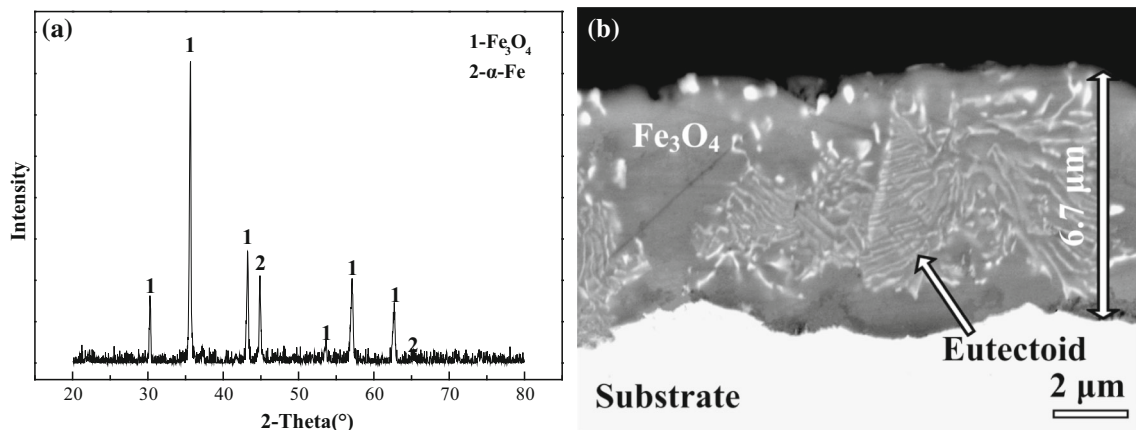


Figure 3 Composition of the oxide scale: **a** XRD pattern and **b** cross-sectional morphology.

Reduction degree and reaction rate

The effect of reduction methods on the reduction degree and reaction rate of the oxide scale in the synthetic atmosphere 20% H₂-Ar is studied. The reduction degree R is calculated by:

$$R = \frac{\Delta W_t}{\Delta W_R} \times 100\% \quad (1)$$

where ΔW_t is the mass loss of the oxide scale in the reduction process at certain time t ; ΔW_R is defined as the mass loss when the sample was isothermally reduced at 1000 °C until no further mass variation with reaction time. The reduction degree of the oxide scale under different methods is shown in Fig. 4. It can be found that the reduction degree is a function of the reaction time, and the reduction degree is enhanced with a delay in the reaction time. The reduction degree of S4 is 41% when the reaction time is 10 min, which is the highest among all methods of single-stage reduction. It is worth noting that the reduction degree of the oxide scale at 500 °C is higher than that at 600 °C and 700 °C. Additionally, it can be seen that the reduction degree of D1 in this interval time of 0–7 min for the reduction reaction is higher than that of the other reduction methods, and the reduction degree of D3 is 85% after a 10 min reaction, which is more than twice as high as S4. Therefore, it is inferred that the reduction methods using “low temperature and high temperature” can play a role in accelerating reduction reaction.

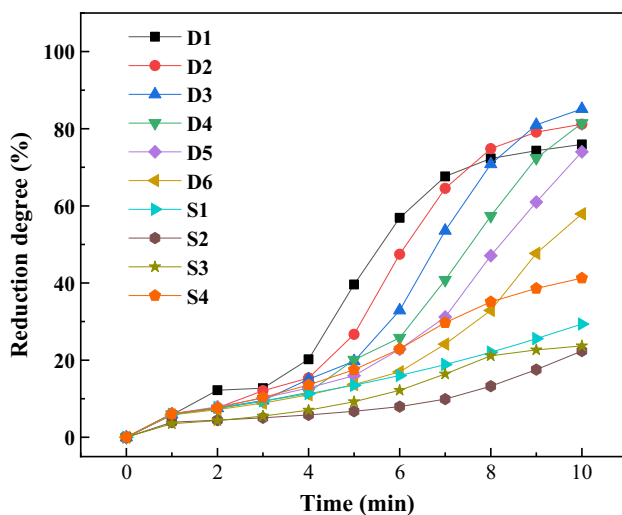


Figure 4 Reduction degree of oxide scale under different reduction methods.

To further clarify and define the influences of the reduction methods on the reaction efficiency, the function of the relationship between the reduction degree and reaction rate over different interval times is analyzed [21]. The reaction rate r is calculated by:

$$r = \frac{dR}{dt} = \frac{\Delta R}{\Delta t} = \frac{R_{t+\Delta t} - R_t}{\Delta t} \quad (2)$$

where ΔR is the reduction degree for different time intervals (Δt). Figures 5 and 6 show the r - R curves of the single-stage reduction method and the double-stage reduction method, respectively. It can be seen that the reaction rate presents an upward trend at 500 °C, as shown in Fig. 5. The reaction rate of the oxide scale during an isothermal reduction at 800 °C is 1.5–2 times higher than that at 500 °C within the reduction degree range of 10–30%. However, the reaction rate is observed to have an inflection point of decrease at the reduction degree of 27% at 800 °C, and it sharply decreases in the reduction degree range of 27–41%. Moreover, Fig. 6 shows the reaction rate curve of the oxide scale under the double-stage reduction methods. The curve of the D1 method is exhibited in Fig. 6a. The reaction rate at 700 °C is the trough in the heating reduction stage, and then the reaction rate sharply increases initially to an isothermal reduction stage at 800 °C; subsequently, it can be found that the inflection point of the reaction rate change occurs at the reduction degree of 39%, and then the reaction rate is soon after observed to show a sharp decline. The variation trend of the reaction rate curve of the D3 method (Fig. 6b) is in

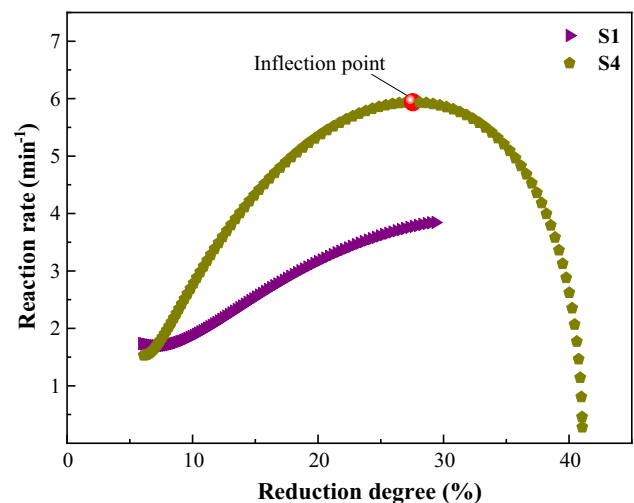


Figure 5 Reaction rate curve of the oxide scale under single-stage reduction method.

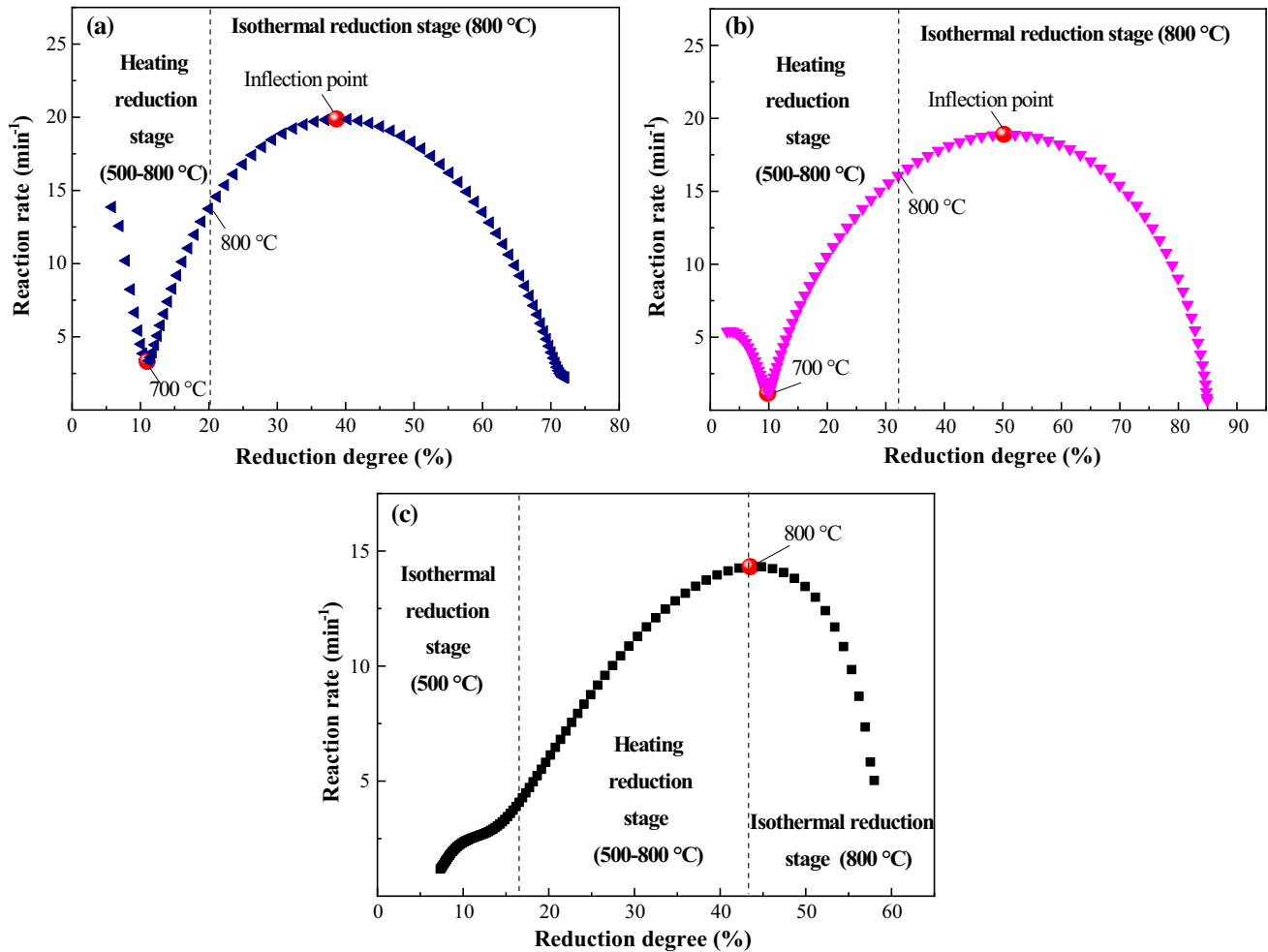


Figure 6 Reaction rate curves of the oxide scale under double-stage reduction method: **a** D1, **b** D3, **c** D6.

agreement with that of D1 method, and the inflection point of the reaction rate decrease is found at the reduction degree of 50%. Figure 6c shows the reaction rate curve of the D6 method. The main differences in the change trend from the other two are the reduction trough disappearing at 700 °C in the heating reduction stage, and then the reaction rate immediately decreases at the end of heating reduction stage, and the inflection point occurs at the reduction degree of 43.5%. By comparing Figs. 5 and 6, the results indicate that the double-stage reduction method causes great improvement of the reaction rate, and the inflection point of decrease for the reaction rate is delayed in comparison with the single-stage reduction method. The parameters of the most efficient reduction in the double-stage methods are isothermal reduction at 500 °C for 3 min combined with 800 °C for 4 min. Considering the demand for a rapid reaction rate in practical

production, the double-stage reduction method is more than sufficient for the reduction process of the oxide scale formed on hot-rolled steel sheet.

Phase composition and cross-sectional morphology

XRD patterns are used to identify the phase composition of the reduction layer under the reduction reaction methods of S1, S4, D3 and D6, as shown in Fig. 7. It can be found that the reduction product of the oxide scale consisted of Fe_3O_4 and $\alpha\text{-Fe}$ under the single reduction method of S1. In the reduction method of S4, the Fe_3O_4 peaks are nearly absent and the phase of the reduction layer mainly consisted of FeO and $\alpha\text{-Fe}$. The Fe_3O_4 peaks disappear and the FeO peaks become weak under the reduction reaction methods of D3 and D6, which are replaced by intensity peaks of $\alpha\text{-Fe}$ due to the removal of a large

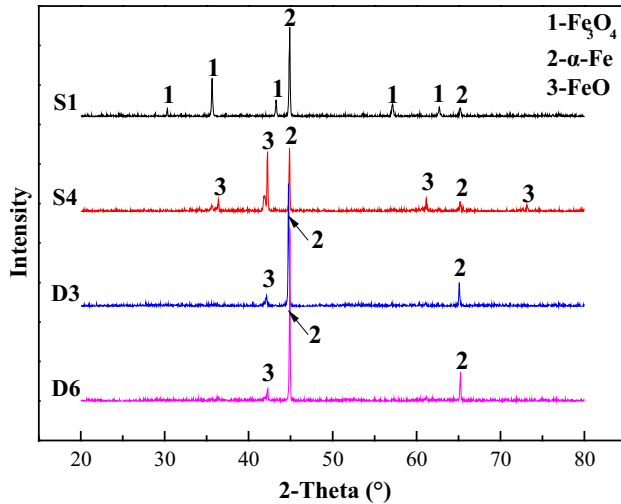


Figure 7 XRD patterns of reduction layer.

amount of oxygen from the oxide scale by gas–solid reduction reaction. Compared with the phase composition of the initial oxide scale in Fig. 3a, the XRD results for the reduction layer indicate that a higher ratio of α -Fe in the reduction layer can be obtained under the double-stage reduction method.

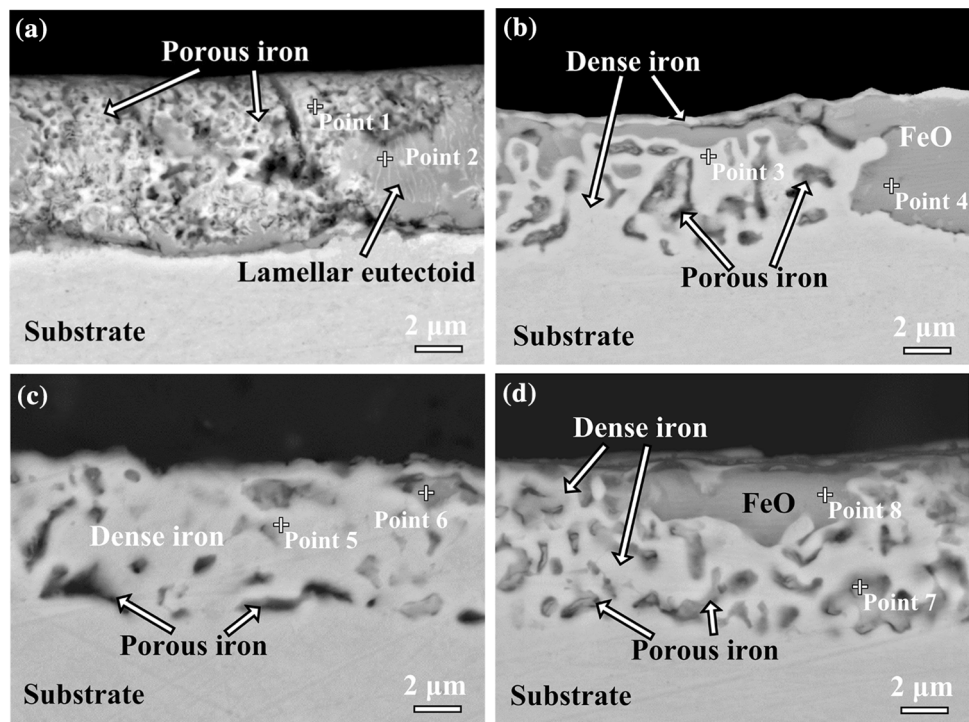
Meanwhile, the cross-sectional morphologies of the reduction layer under different reduction methods are shown in Fig. 8, and the elemental composition at different positions is listed in Table 2. Combined

Table 2 Elemental composition at different positions of cross section of the reduction layer in Fig. 8

Position	Mass percent/mass%		Position	Mass percent/mass%	
	Fe	O		Fe	O
Point 1	93.24	6.76	Point 5	100	–
Point 2	73.80	26.20	Point 6	96.98	3.02
Point 3	100	–	Point 7	95.88	4.12
Point 4	79.42	20.58	Point 8	80.94	19.06

with the XRD results of the reduction layer, it can be inferred that the reduction layer is mainly composed of porous iron and the remaining eutectoid structure ($\text{Fe}_3\text{O}_4/\alpha\text{-Fe}$) after the reduction method of S1, as seen in Fig. 8a, and the mass percent of oxygen in porous iron and eutectoid is 6.76% and 26.20%, respectively. In the reduction method of S4, oxygen cannot be measured in reduced dense iron, while the mass percent of oxygen in unreduced Fe oxides is 20.58%. Figure 8b shows that the external side of the reduction layer is a dense iron layer, and the remaining Fe oxides are surrounded by dense iron and porous iron that has a larger diameter than that in the reduction layer with the S1 method. The oxide scale is completely reduced to dense iron and a small

Figure 8 Cross-sectional morphologies of reduction layer under different reduction methods: a S1, b S4, c D3, d D6.



amount of porous iron under the double-stage reduction method of D3, the mass percent of oxygen in porous iron is 3.02%, and then no remaining bulk Fe oxides in the reduction layer are observed in Fig. 8c. Compared with the D3 method, Fig. 8d shows a small quantity of bulk Fe oxides with oxygen mass percent of 19.06%; dense iron and larger amounts of porous iron form in the reduction layer during the D6 method. It is worth noting that the morphologies of the reduction layers are entirely different although the reaction time of the above-mentioned reduction methods is all around 10 min. The main reason may be the phase transformation of the oxide scale and the differences in the restrictive links of the reduction reaction under different reduction temperatures, which will be highlighted in the Discussion section.

Surface morphology

Figure 9 shows the surface morphologies of the initial oxide scale and the reduction layer. The surface morphology of the initial oxide scale is very smooth, and there was not a large amount of crack on the surface (Fig. 9a), and there are no obvious defects, such as oxides breakaway and a large amount of cracks. After isothermal reduction at 500 °C for 10 min, hydrogen atoms adsorb on the surface of oxide scale and then react with oxygen atoms in the Fe oxides to generate water which desorbs from the surface in the form of vapor. Figure 9b shows a number of pores form on the surface due to a large number of oxygen atoms vacancies gather together after reduction reaction. However, the dense iron with grain characteristics is observed on the surface of the reduction layer after isothermal reduction at 800 °C for 10 min, as seen in Fig. 9c. In the double-stage reduction method of D3, it can be found that the surface of the reduction layer is dense iron with grain characteristics (seen in Fig. 9d), and then a certain amount of micro-cracking forms due to volume contraction or stress relaxation, and the micro-cracking width is 0.8–1.4 μm. Figure 9e shows the surface morphology under the reduction reaction method of D6, which is in general agreement with D3, and the micro-cracking width is 1.4–1.6 μm.

Discussion

Phase transformation of the oxide scale

To analyze the phase transformation of the oxide scale under the heating process before the reduction reaction, the oxide scale was heated to the target temperature (500 °C and 800 °C) at a rate of 60 °C/min, and then they were immediately cooled to room temperature at a rate of 40 °C/min to preserve the structure of the oxide scale. The whole heating process is completed under the protection of Ar gas. XRD patterns and the cross-sectional morphologies of the oxide scale after the above-mentioned experiments are shown in Fig. 10. The oxide scale consists of Fe₃O₄ and the eutectoid structure (Fe₃O₄/α-Fe) during heat treatment at 500 °C, as shown in Fig. 10a, b, which is in agreement with the phase composition and morphology of the initial oxide scale in Fig. 3. This result indicates that the structure of the oxide scale can remain unchanged at 500 °C. However, Fe₃O₄ and the eutectoid structure (Fe₃O₄/α-Fe) of the initial oxide scale completely transform to FeO with the heating temperature rising to 800 °C, as shown in Fig. 10c, d. To clarify the cause of the phase transformation of the oxide scale, the Fe–O binary equilibrium phase diagram is shown in Fig. 11. The diagram shows that 570 °C is the critical temperature of FeO thermodynamically stable. Fe₃O₄ and the α-Fe gradually transform to FeO when the temperature is higher than 570 °C in the heating process. In the process of phase transformation, iron atoms act as the reducing agent, diffuse into the lattice of Fe₃O₄, and turn it into FeO of lower valence. The chemical reaction equation is as follows:



Similar results have also appeared in previous studies [10, 14, 20]. It can be seen that the oxide scale is comprised of layered structures, and the order from outside to inside is Fe₂O₃, Fe₃O₄, FeO and the Fe₃O₄/α-Fe eutectoid structure, which will completely change to FeO during heat treatment above 570 °C. The phase transformation of the oxide scale under the heating process can be used to explain the difference of the reduction layer structure between the reduction methods of S1 and S4. Moreover, the crystal structure of Fe oxides in the oxide scale has also been characterized and analyzed by TEM and EBSD in previous studies [22–24]. These results

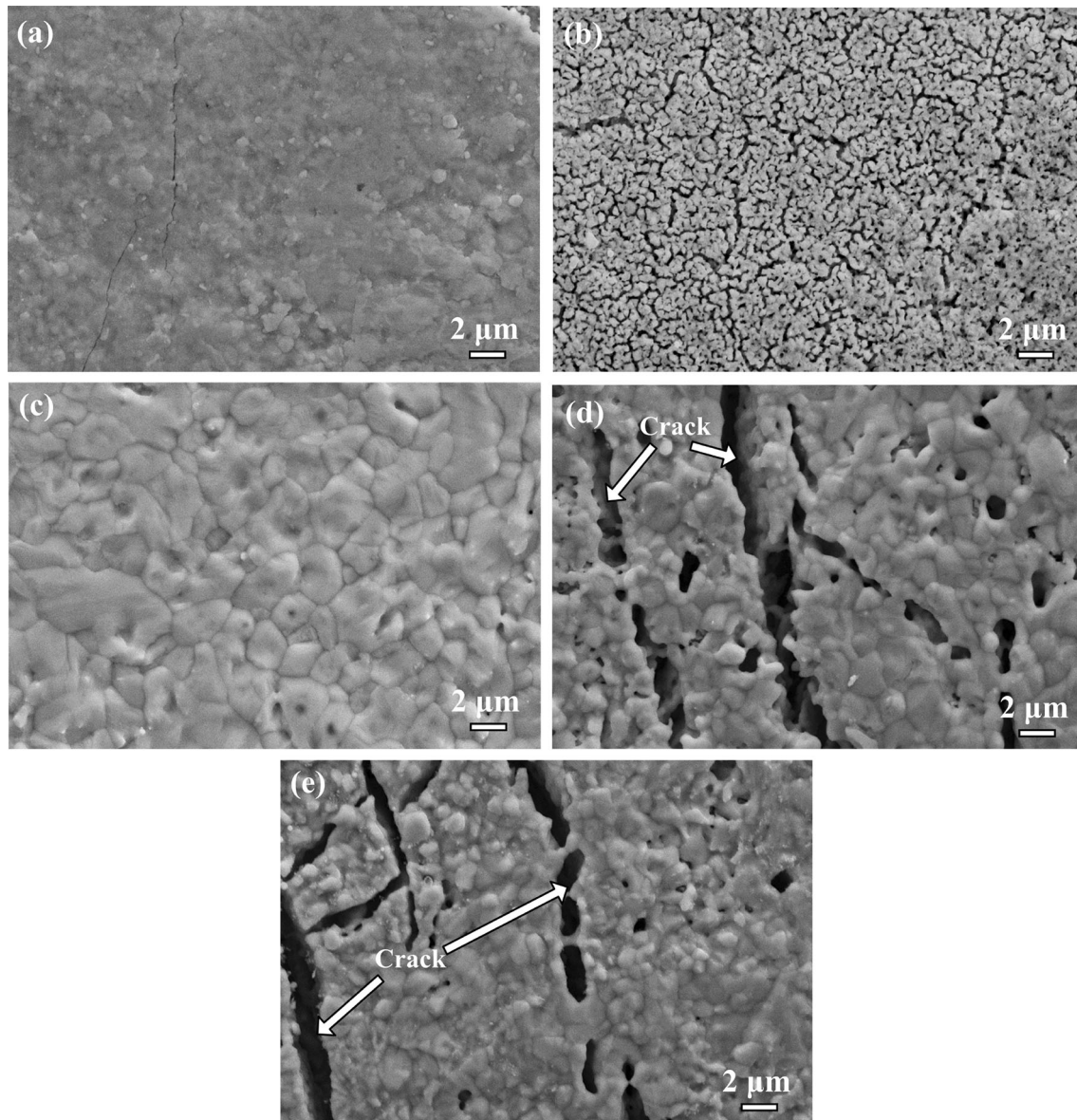


Figure 9 Surface morphology of oxide scale and reduction layer: **a** oxide scale, **b** S1, **c** S4, **d** D3, **e** D6.

indicate that the eutectoid structure in the oxide scale exhibited a type of lamellar structure containing Fe_3O_4 and $\alpha\text{-Fe}$ of alternative distribution and that contained many phase interfaces in it. However, FeO forms a type of columnar grain that grows perpendicular to the metal substrate; the grain size of FeO is large, and only a few grain boundaries can act as diffusion channels for hydrogen and water vapor. In the initial stage of reduction at $800\text{ }^\circ\text{C}$, the reduced metallic iron around FeO completely changes into a dense iron layer. With the increase in the reaction time, the diffusion of the reducing gas in solid is suppressed due to the increase in reduction layer

thickness, and nucleation and growth of new phase. Therefore, the reaction rate under S4 method after the reduction degree of 27% decreased sharply, as shown in Fig. 5. Combining the previous research results and this study, it can be inferred that FeO is the most difficult of the Fe oxides to be reduced.

Restrictive link of reduction reaction

The reduction reaction between hydrogen and the oxide scale is a complex multiphase gas–solid reaction. The whole reduction process can be summarized as three major restrictive links: external

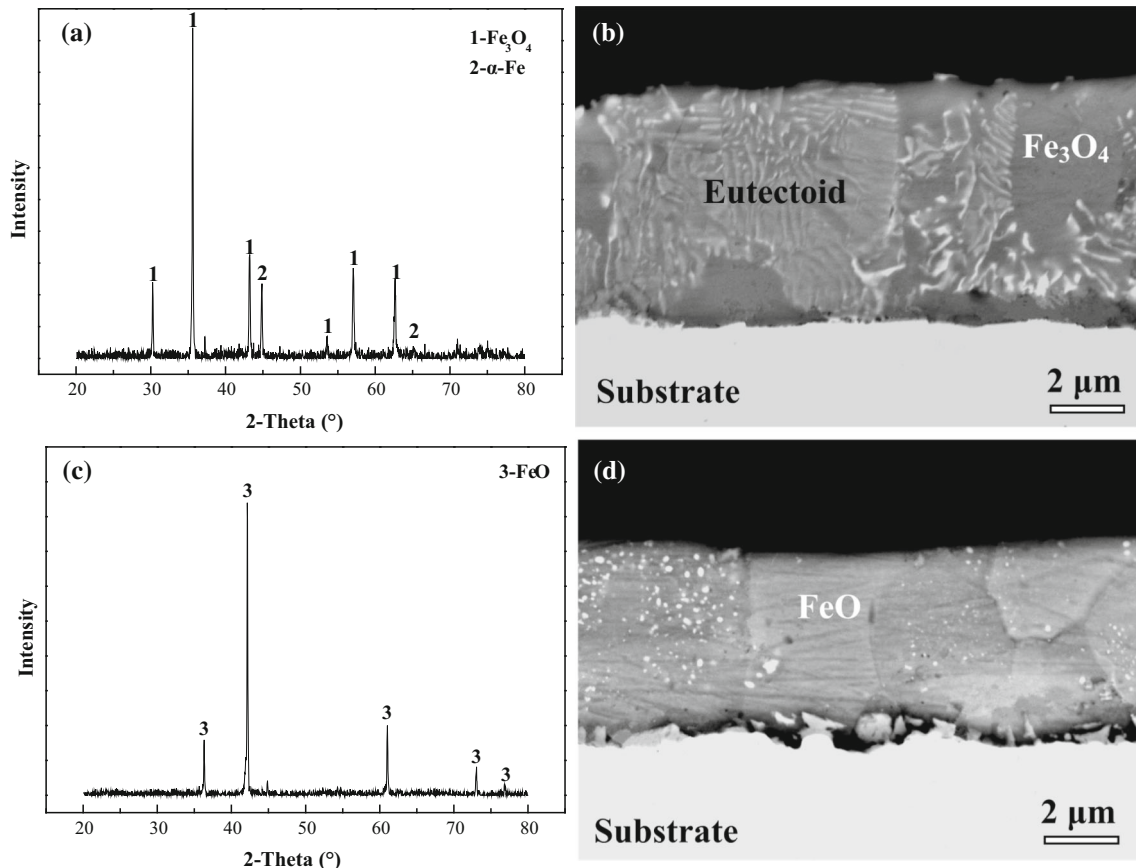


Figure 10 XRD patterns and cross-sectional morphologies of the oxide scale after heating at **a, b** 500 °C; **c, d** 800 °C.

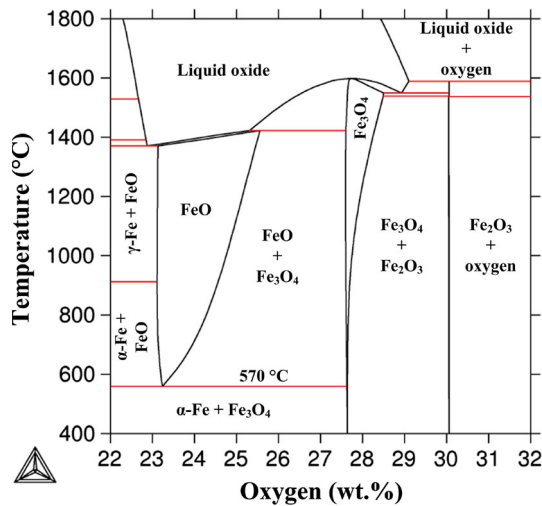
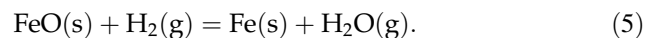
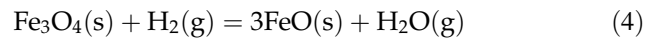


Figure 11 Fe–O binary equilibrium phase diagram.

diffusion, internal diffusion and interfacial reaction. The interfacial reaction between gases and solids includes adsorption and desorption of gas at phase interface, interface reaction and reconstruction of new phase lattices. The total rate of the reaction

process is related to the rate of the main restrictive link of the reduction reaction or the resistance within it, which depends on the rate of the slowest link under the reduction condition.

In the gas–solid chemical reaction, the Fe oxides present a principle of step-by-step transformation during reduction reactions above 570 °C. The conversion of Fe₃O₄ to metallic iron requires two steps in the reduction hydrogen environment. The chemical reaction equation may be represented by:



However, the different transformation orders are found when the reduction temperature is below 570 °C. The chemical reaction equation between Fe₃O₄ and H₂ is as follows:

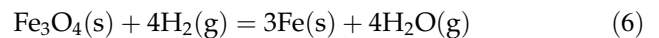


Figure 5 suggests that the reaction rate presents a rising tendency without the inflection point of

decrease during the whole reaction process of reduction at 500 °C for 10 min. Based on the previous researches [25, 26], it can be found that the structure of reduction layer is the key to determine the rate of reduction reaction. After reduction at 500 °C, the reduction product of the oxide scale is the porous iron which can be described as a continuous dendritic structure, as shown in Fig. 12. It can be found that the pore tips are the location of the interface reaction for the elementary mass transport and chemical reactions. The Fe oxides at the pore tip can be reduced first due to the direct contact with the internal diffusion of the reduction gas and the high thermodynamic driving force at the dendrite tip. Subsequently, a large number of the porous iron with continuous dendritic structure form in the oxide scale with the reaction time, which plays a positive effect on the adsorption of hydrogen and the desorption of water vapor at phase interface, and nucleation and growth of new phase.

In the initial stage of isothermal reduction at 800 °C, the reaction rate increases first and decreases afterward with the increase in reduction degree, as shown in Fig. 5. It is considered that the residual Fe oxides are completely surrounded by the dense-reduced iron, and then the reduction layer becomes thicker, and the internal diffusion resistance increases with the extension of the reduction time, which results in the gradually decrease in reduction efficiency. The schematic illustration of the dense reduction iron formation in the oxide scale under the

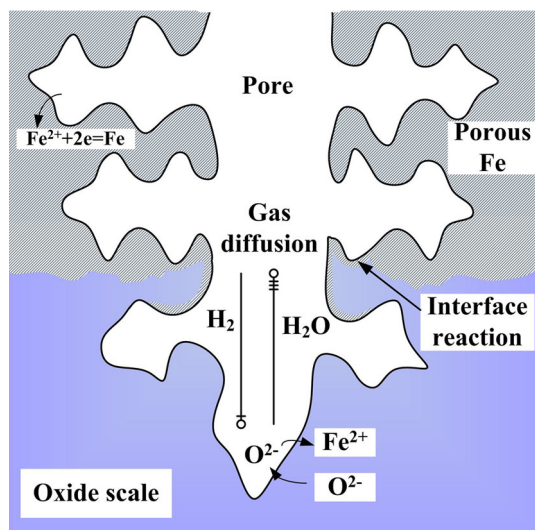


Figure 12 Schematic illustration of reduced porous iron of continuous dendritic structure.

isothermal reduction at 800 °C is described in Fig. 13. Meanwhile, the eutectoid structure in the initial oxide scale will transform completely to FeO at the heating stage (seen in Fig. 10d). Therefore, the reduction reaction of the oxide scale at 800 °C can also be seen as the reduction process of FeO, which is divided into three stages: incubation, acceleration and decay. In the incubation stage, the reaction begins with some active points caused by dislocations, vacancies and other defects on the surface of oxide scale due to the more easily of hydrogen atoms diffuse at the defects than that at complete lattices. Subsequently, the reduction reaction enters the acceleration stage. The content of reduced pure iron increases gradually with the chemical reaction from the surface of the oxide scale to its interior. It can be found that a phase interface between the old phase of the reactant and the new phase of reducing product can be observed clearly. The phase interface expands inward continuously during the reduction reaction, which plays a catalytic role in the adsorption of hydrogen and the interface reaction and then results in the increase in reaction rate with the expansion of the interface. Additionally, the interface between the oxide scale and the steel substrate will also be reduced at an earlier time due to the larger lattice distortion, the higher energy and the smaller diffusion activation energy at this location. At the same time, the content of iron atoms in the oxide scale near the steel substrate is higher, and fewer oxygen atoms at the interface can easily be carried away by hydrogen to form cavities. Finally, the reduction reaction enters the decay stage due to the shrink of the interface between the FeO and reduced pure iron, resulting in the specific surface area of FeO declining when the front edge of the reaction interface reaches the limit. The diffusion of hydrogen and water vapor through the dense pure iron layer is hindered, and then there is a gradual decrease in the reaction rate with increasing reaction time. Consequently, it can be inferred that the restrictive link of the reaction rate of the oxide scale at 800 °C is internal diffusion.

Based on the above-mentioned restrictive links of the reduction reaction at 500 °C and 800 °C, the advantages of the reduction reaction at different temperatures can be summarized. The advantage of a reduction reaction at 500 °C is the internal diffusion, and the advantage of a reduction reaction at 800 °C is the interfacial reaction. In this study, the double-stage reduction method of “low temperature and high

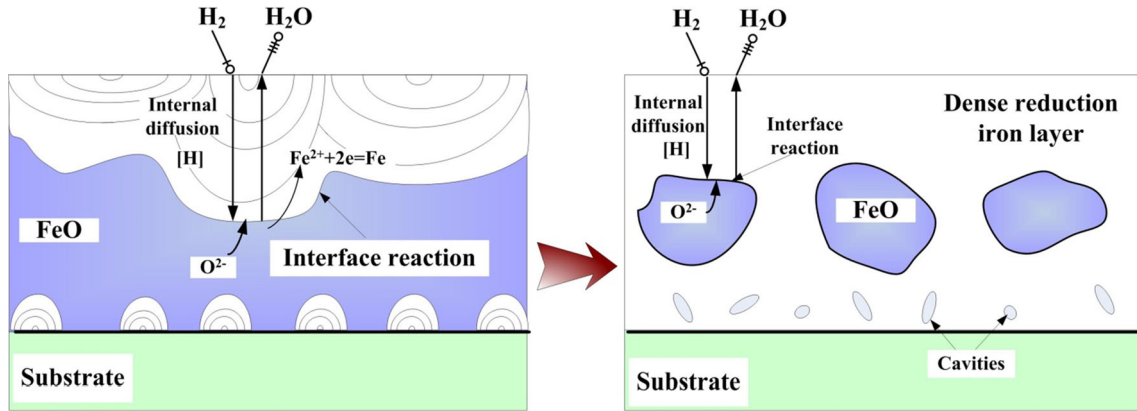


Figure 13 Schematic illustration of formation of dense reduction iron.

temperature” is proposed, which combines the advantages of reduction reactions at 500 °C and 800 °C. The most prominent performance of the double-stage method in the experimental results is that the reduction degree is significantly increased and the decrease inflection point of the reduction reaction rate is delayed compared with the traditional single-stage reduction method, as seen in Figs. 4, 5 and 6. In this context, the mechanism illustrated of the double-stage reduction method can be shown in Fig. 14.

The mechanism of the double-stage model causing the increase in reduction degree can be divided into the following aspects. Firstly, the oxide scale is partially reduced at 500 °C, and the oxygen atoms in the initial oxide scale are removed through the gas–solid chemical reaction, which leads to the appearance of a large number of vacancies in the lattice of Fe oxides. Meanwhile, the number of vacancies increases continuously during the heating reduction process of

500–800 °C, and then the pores form in the oxide scale, which makes it impossible to provide enough oxygen atoms during the solid-state phase transformation of the $\text{Fe}_3\text{O}_4/\alpha\text{-Fe}$ eutectoid structure to FeO (as shown in Eq. 3), and then a certain amount of bulk FeO will exist in the oxide scale before reduction at 800 °C. Secondly, the reduction products of the oxide scale during the isothermal reduction at 500 °C are the porous iron of continuous dendritic structure, and a large number of pores can be connected together, which provides the diffusion channels for the adsorption of hydrogen and the desorption of water vapor at the gas–solid interface. At 800 °C, the new phase starts to gradually nucleate and grow causing the formation of micro-cracking on the surface due to volume contraction and stresses release. The micro-cracking also plays a role in accelerating gas diffusion. Therefore, the mechanism of the double-stage reduction method reveals that the phase transformation of oxide scale and the structure reduction

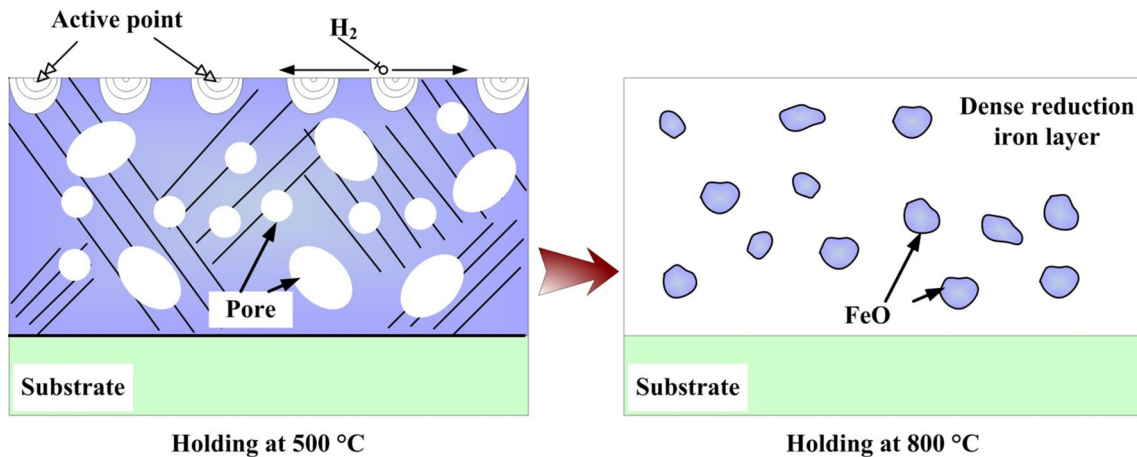


Figure 14 Reaction mechanism of double-stage reduction method.

layer is precisely controlled by the reasonable optimization of reduction temperature, which is the main key to improve reduction efficiency of the oxide scale.

Conclusions

A novel high-efficiency reduction method of the oxide scale formed on hot-rolled low-carbon steel has been proposed in this study. The reduction degree and reaction rate of the oxide scale during the double-stage reduction method of “low temperature and high temperature” are significantly higher than that during the traditional single reduction method. The optimal parameters of the double-stage method are isothermal reduction at 500 °C for 3 min combined with 800 °C for 4 min. The highest reduction degree can achieve 85%, the decline inflection point of the reaction rate is delayed to the reduction degree of 50%, and the phase composition of the reduction product is mainly reduced iron without Fe oxides under the optimal parameters. The double-stage reduction method is a method that combines the advantages of the oxide scale reduction at 500 °C and 800 °C. The mechanism of the oxide scale reduction under the double-stage method can be divided into two main aspects. In the reduction stage of low temperature at 500 °C, a large amount of pores are formed in the oxide scale due to the removing of oxygen atoms in Fe_3O_4 by the gas–solid reduction reaction, which can effectively inhibit the phase transformation of the eutectoid structure $\text{Fe}_3\text{O}_4/\alpha\text{-Fe}$ to FeO during the subsequent heating process. When it enters the reduction stage of high temperature at 800 °C, the micro-cracking on the surface of the oxide scale and the pores at the interior of the oxide scale are connected together to form diffusion channels for hydrogen and water vapor, which play a positive role for the interfacial reaction efficiency of residual Fe oxides around the pores.

Acknowledgements

The work was supported by the National Nature Science Foundation of China (Grant No. U1660117); the China Postdoctoral Science Foundation (Grant No. 2019M651132); and the Fundamental Research Funds for the Central Universities (Grant No. N180703010).

References

- [1] Gutierrez-Platas JL, Artigas A, Monsalve A, García-Gómez NA, García-Rincón O, De la Garza-Garza M, Pérez-González FA, Colás R, Garza-Montes-de-Oca NF (2018) High-temperature oxidation and pickling behaviour of HSLA steels. *Oxid Met* 89:33–48
- [2] Ding JW, Tang B, Li MY, Feng XF, Fu FL, Bin LY, Huang SS, Su W, Li DN, Zheng LC (2017) Difference in the characteristics of the rust layers on carbon steel and their corrosion behavior in an acidic medium: limiting factors for cleaner pickling. *J Clean Prod* 142:2166–2176
- [3] Wu G, Guan C, Tan N, Zhang J (2018) Effect of hot rolled substrate of hydrogen reduction on interfacial reaction layer of hot-dip galvanizing. *J Mater Process Technol* 259:134–140
- [4] Lin SN, Huang CC, Wu MT, McDermid JR, Hsieh KC (2017) Studies of interface reactions between zinc and reduced red scale on a Mn/Si dual phase steel. *J Alloy Compd* 729:257–265
- [5] Li ZF, He YQ, Cao GM, Tang JJ, Zhang XJ, Liu ZY (2017) Effects of Al contents on microstructure and properties of hot-dip Zn–Al alloy coatings on hydrogen reduced hot-rolled steel without acid pickling. *J Iron Steel Res Int* 24:1032–1040
- [6] Jing YA, Zang X, Shang Q, Qin Y, Li Y, Song B (2015) The evolution of surface morphologies and microstructures during cold rolling after hydrogen reduction. *J Mater Process Technol* 219:303–313
- [7] Primavera A, Cattarino S, Pavlicevic M (2007) Influence of process parameters on scale reduction with H_2 . *Ironmak Steelmak* 34:290–294
- [8] Guan C, Li J, Tan N, Zhang SG (2016) Continuous reduction of the oxide scale of hot-rolled steel strip in hydrogen. *Ironmak Steelmak* 43:739–743
- [9] Jing YA, Yuan YM, Yan XL, Zhang L, Sha MH (2017) Decarburization mechanism during hydrogen reduction descaling of hot-rolled strip steel. *Int J Hydrog Energy* 42:10611–10621
- [10] Tanei H, Kondo Y (2012) Effect of initial scale structure on transformation behavior of wüstite. *ISIJ Int* 52:105–109
- [11] Chen RY (2017) Mechanism of iron oxide scale reduction in 5% $\text{H}_2\text{-N}_2$ gas at 650–900 °C. *Oxid Met* 88:687–717
- [12] Saeki I, Ikeda T, Ohno K, Sato T, Kurosawa S (2011) Reduction of oxide scales formed on low carbon steel sheet in synthesized combustion gas. *Tetsu-to-Hagane* 97:12–18
- [13] Moukassi M, Steinmetz P, Dupre B, Gleitzer C (1983) A study of the mechanism of reduction with hydrogen of pure wüstite single crystals. *Metall Trans B* 14:125–132

- [14] He YQ, Jia T, Li ZF, Cao GM, Liu ZY, Li J (2016) Isothermal reduction of oxide scale on hot-rolled, low-carbon steel in 10 pct H₂-Ar. *Metall Mater Trans A* 47:4845–4852
- [15] Guan C, Li J, Tan N, He YQ, Zhang SG (2014) Reduction of oxide scale on hot-rolled steel by hydrogen at low temperature. *Int J Hydrog Energy* 39:15116–15124
- [16] Badin V, Diamanti E, Forêt P, Darque-Ceretti E (2016) Early steps of pore formation during stainless steel oxides reduction with hydrogen at 1373 K (1100 °C). *Metall Mater Trans B* 47:1445–1452
- [17] Liu XJ, Cao GM, He YQ, Yang M, Liu ZY (2014) Reduction of oxide scale with hydrogen. *J Iron Steel Res Int* 21:24–29
- [18] Li ZF, Cao GM, Lin F, Sun XZ, He YQ, Liu ZY (2017) Effect of cold rolling before hydrogen reduction on reduction behavior and morphologies of oxide scale on hot-rolled low-carbon steel. *ISIJ Int* 57:2034–2041
- [19] Shi J, Wang DR, He YD, Qi HB, Gao W (2008) Reduction of oxide scale on hot-rolled strip steels by carbon monoxide. *Mater Lett* 62:3500–3502
- [20] Ding D, Peng H, Peng W, Yu Y, Wu G, Zhang J (2017) Isothermal hydrogen reduction of oxide scale on hot-rolled steel strip in 30 pct H₂-N₂ atmosphere. *Int J Hydrog Energy* 42:29921–29928
- [21] Li W, Fu GQ, Chu MS, Zhu MY (2017) Effect of reducing conditions on swelling behavior and mechanism of Hongge vanadium titanomagnetite-oxidized pellet with hydrogen-rich gases. *Int J Hydrog Energy* 42:24667–24674
- [22] Lin SN, Huang CC, Wu MT, Wang WL, Hsieh KC (2017) Crucial mechanism to the eutectoid transformation of wüstite scale on low carbon steel. *Steel Res Int* 88:1700045
- [23] Yu XL, Jiang ZY, Zhao JW, Wei DB, Zhou J, Zhou CL, Huang QX (2016) The role of oxide-scale microtexture on tribological behaviour in the nanoparticle lubrication of hot rolling. *Tribol Int* 93:190–201
- [24] Basabe VV, Szpunar JA (2004) Growth rate and phase composition of oxide scales during hot rolling of low carbon steel. *ISIJ Int* 44:1554–1559
- [25] Hayes PC (2010) Stability criteria for product microstructures formed on gaseous reduction of solid metal oxides. *Metall Mater Trans B* 41:19–34
- [26] Matthew SP, Cho TR, Hayes PC (1990) Mechanisms of porous iron growth on wustite and magnetite during gaseous reduction. *Metall Trans B* 21:733–741

Publisher's Note Springer Nature remains neutral with regard to jurisdictional claims in published maps and institutional affiliations.